

Review

A Global Review of Progress in Remote Sensing and Monitoring of Marine Pollution

Jingwu Ma ^{1,2,3}, Renfeng Ma ^{3,4,5,*} , Qi Pan ⁴, Xianjun Liang ⁶, Jianqing Wang ⁷ and Xinxin Ni ⁸

- ¹ Key Laboratory of Ocean Space Resource Management Technology of Ministry of Natural Resources, Zhejiang Institute of Marine Sciences, Hangzhou 310012, China; majingwu12@163.com
- ² Land Consolidation and Rehabilitation Center, Wenzhou Bureau of Natural Resources and Planning, Wenzhou 325027, China
- ³ Ningbo University Donghai Academy & Zhejiang Ocean Development Think Tank Alliance, Ningbo 315211, China
- ⁴ Department of Geography and Spatial Information Techniques, Ningbo University, Ningbo 315211, China; 2011087072@nbu.edu.cn
- ⁵ Zhejiang Collaborative Innovation Center & Ningbo Universities Collaborative Innovation Center for Land and Marine Spatial Utilization and Governance Research, Ningbo University, Ningbo 315211, China
- ⁶ Ningbo Junzhi Engineering and Environmental Consulting Co., Ltd., Ningbo 315211, China; nbuandrew@163.com
- ⁷ Ningbo Institute of Oceanography, Ningbo 315832, China; wangjq@nbio.org.cn
- ⁸ Department of International Hotel Management at Qiandaohu, Tourism College of Zhejiang China, Hangzhou 311231, China; nixinxin@tourzj.edu.cn
- * Correspondence: marenfeng@nbu.edu.cn

Abstract: With the rapid development of urbanization and industrialization, human activities have caused marine pollution in three ways: land source, air source, and sea source, leading to the problem of marine environments. Remote sensing, with its wide coverage and fast and accurate monitoring capability, continues to be an important tool for marine environment monitoring and evaluation research. This paper focuses on the three types of marine pollution, namely marine seawater pollution, marine debris and microplastic pollution, and marine air pollution. We review the application of remote sensing technology methods for monitoring marine pollution and identify the limitations of existing methods. Marine seawater pollution can be effectively monitored by remote sensing technology, especially where traditional monitoring methods are inadequate. For marine debris and microplastic pollution, the monitoring methods are still in the early stages of development and require further research. For marine air pollution, more air pollution parameters are required for accurate monitoring. Future research should focus on developing marine remote sensing with data, technology, and standard sharing for three-dimensional monitoring, combining optical and physical sensors with biosensors, and using multi-source and multi-temporal monitoring data. A marine multi-source monitoring database is necessary to provide an immediately available basis for coastal and marine governance, improve marine spatial planning, and help coastal and marine protection.

Keywords: marine environmental monitoring; governance; marine pollution; coastal zone management



Citation: Ma, J.; Ma, R.; Pan, Q.; Liang, X.; Wang, J.; Ni, X. A Global Review of Progress in Remote Sensing and Monitoring of Marine Pollution. *Water* **2023**, *15*, 3491. <https://doi.org/10.3390/w15193491>

Academic Editors: Camilo M. Botero, Celene B. Milanés and Daniel O. Suman

Received: 24 August 2023

Revised: 25 September 2023

Accepted: 26 September 2023

Published: 6 October 2023



Copyright: © 2023 by the authors. Licensee MDPI, Basel, Switzerland. This article is an open access article distributed under the terms and conditions of the Creative Commons Attribution (CC BY) license (<https://creativecommons.org/licenses/by/4.0/>).

1. Introduction

The ocean is an important environment for humans, and its various types and scales of currents result in the distribution of liquid and three-dimensional resources, which form an important and unique system of marine resources and environment. The ocean is abundant in biological resources, mineral resources, energy, and other resources, and it is attracting increasing attention from the academic circle and industry. The rapid development of industrialization and urbanization has led to a concentration of human activities along coastlines, resulting in the degradation of coastal bays, marine resources, and the environment [1].

Generally, the coastal natural shoreline and coastal mudflat wetlands have been continuously reduced, the area of mangroves and coral reefs has been greatly reduced, and the marine ecological environment has been polluted. The situation is becoming increasingly serious, with increasing eutrophication of seawater and frequent occurrences of marine ecological disasters such as brown tides, green tides, and red tides posing a serious threat to migratory waterfowl and marine biodiversity. Meanwhile, the above environmental pollution, biological extinction, and natural disasters have posed a threat to the sustainable development of the coastal and marine environment. Dissolved organic matter from sewage treatment plants, humus from farmland, anthropogenic shoreline erosion, and the removal of native vegetation can cause significant increases in turbidity in coastal waters [2]. For example, NASA satellite imagery has shown that the water quality of Florida's Tampa Bay decreases in the winter months compared to the summer. More particles suspended in the water, a measure called turbidity, show up as yellow, orange, and red in December (a) than in July (b) due to seasonal freshwater discharge from nearby rivers and runoff into the bay, which carry nutrients (Figure 1). Hence, marine pollution monitoring is of great significance in terms of both theoretical and practical value [3–5]. Marine environment monitoring is an essential step in maintaining the quality of the marine environment and securing its ecology, and it is crucial for achieving sustainable marine development.

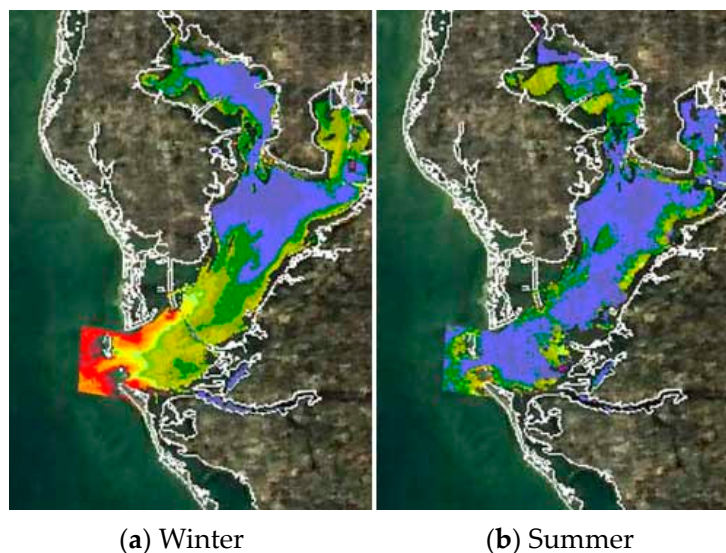


Figure 1. Water quality of Florida's Tampa Bay decreases (Picture source NASA/USF).

Remote sensing plays a crucial role in marine monitoring, including the ecological monitoring of wetland, mangrove, coral reefs, and other key organisms (Figures 2 and 3), the environmental disaster monitoring of oil spills and red tides, the mapping of mesoscale coastlines, the measurement of chlorophyll-a, suspended sediment concentration, seawater temperature in offshore areas, and the automatic recognition of key targets such as dams, breeding areas, buildings, ports, bridges, and ships [6–8].

Based on a search of the Web of Science core collection from 2000 by using the keyword "marine remote sensing," it can be seen that marine remote sensing monitoring is a crucial aspect of marine ecological monitoring (Table 1). Remote sensing monitoring has been of interest to scholars from institutions that have published a number of important papers in this field, such as the Woods Hole Oceanographic Institution, the University of Washington, the University of California, San Diego, Oregon State University, the Plymouth Marine Laboratory, the First, Second, and Third Institutes of Oceanography, the Marine Environmental Monitoring Center, the Marine Technology Center, the Tianjin Marine Environmental Monitoring Center Station, the Ocean University of China, and Xiamen University in China. Meanwhile, government agencies around the world, such as NASA, NOAA, CNRS, and the Canadian Department of Fisheries and Oceans, invest heavily in research in this field.

Meanwhile, NASA, NOAA, and other institutes have established specific research directions in marine remote sensing technology for marine research and also collaborate with universities, whose research not only focuses on marine pollution monitoring, oil spills, dissolved organic carbon, coral issues, and thermal pollution [9–13], but also large-scale marine currents and air-sea interactions. For example, Chinese relevant institutes have specially established a research department in the field of marine remote sensing. The Second Institute of Oceanography of the Ministry of Natural Resources has taken the lead in conducting research on seawater color remote sensing in China and has achieved fruitful results in the mechanism and algorithm of seawater color remote sensing monitoring, as well as the development of domestically produced software system platforms. Relevant units such as the National Satellite Ocean Response Center and the North China Sea Administration of the Ministry of Natural Resources have all implemented operational monitoring applications for offshore oil spills. Furthermore, the Copernicus program also made a lot of contributions, whose program is the Earth observation component of the European Union’s Space program, which offers information services that draw from satellite Earth observation and in-situ (non-space) data. Amounts of global data from satellites and ground-based, airborne, and seaborne measurement systems provide information to help service providers, public authorities, and other international organizations improve European citizens’ quality of life and beyond. And organizations such as USEPA and US IOOS are monitoring exhaust from ships. University of Delaware professors have used remote sensing technology to monitor exhaust from ships.

Table 1. The top 10 related institutes of marine remote sensing monitoring and their research directions.

Research Institute	Number of Paper	Country/Region	Related Laboratory	Research Direction
National Aeronautics and Space Administration	1506	United States	/	Sea level rise monitoring; Marine ecosystem research; Marine currents motion research
National Oceanic and Atmospheric Administration	1276	United States	Pacific Marine Environment Laboratory	Climate-weather research; Marine ecosystem research; Ocean and coastal evolution research
			Global Monitoring Laboratory	Greenhouse gases and carbon cycle research; Changes in clouds, aerosols and surface radiation research; Recovery of stratospheric ozone research
Chinese Academy of Sciences	1028	China	Digital Earth Key Laboratory	Frontier theory and technology of earth observation research; Earth big data science and methods research; Digital earth science and platform research; Global environmental resources spatial information system research
			Key Laboratory of Infrared Detection and Imaging Technology	High-resolution infrared imaging technology research; Hyperspectral imaging technology research; Weak target detection technology research; High quantitative remote sensing detection technology research
California Institute of Technology	853	United States	Linde Center	Earth climate change research [14]; Pollution impact research; Carbon dioxide changes research
University of Washington	617	United States	Applied Physics Laboratory- Air-sea interaction and remote sensing	Sea-air exchange research; Coastal research; Sensor research; Wave research

Table 1. Cont.

Research Institute	Number of Paper	Country/Region	Related Laboratory	Research Direction
University of Maryland	576	United States	Earth System Science Interdisciplinary Center (cooperation with NASA)	Climate variability and change research; Atmospheric composition and processes research; Global carbon cycle research; Global water cycle research
University of California, San Diego	546	United States	Scripps Institution of Oceanography	Collect and process data on the Earth, oceans and atmosphere by cameras, lasers and various electromagnetic sensors
University of Colorado	476	United States	Mortenson Center in Global Engineering	Sustainable water treatment system research; Field and remote sensing research; Infrastructure resilience and disaster recovery research
University of Miami	445	United States	Earth Science and Observation Center, Institute for Research in Environmental Sciences	Analysis of remote sensing data, validation of data
Woods Hole Oceanographic Institution	385	United States	Upper Ocean Dynamics Laboratory	Experimental studies on coastal circulation processes and ocean-atmosphere interactions during the hurricane
			Claisen Laboratory	Studies on air-sea interactions and their impact on weather and climate through a wide range of measured and remote sensing data

Note: The laboratory information is compiled from the official websites of various organizations.

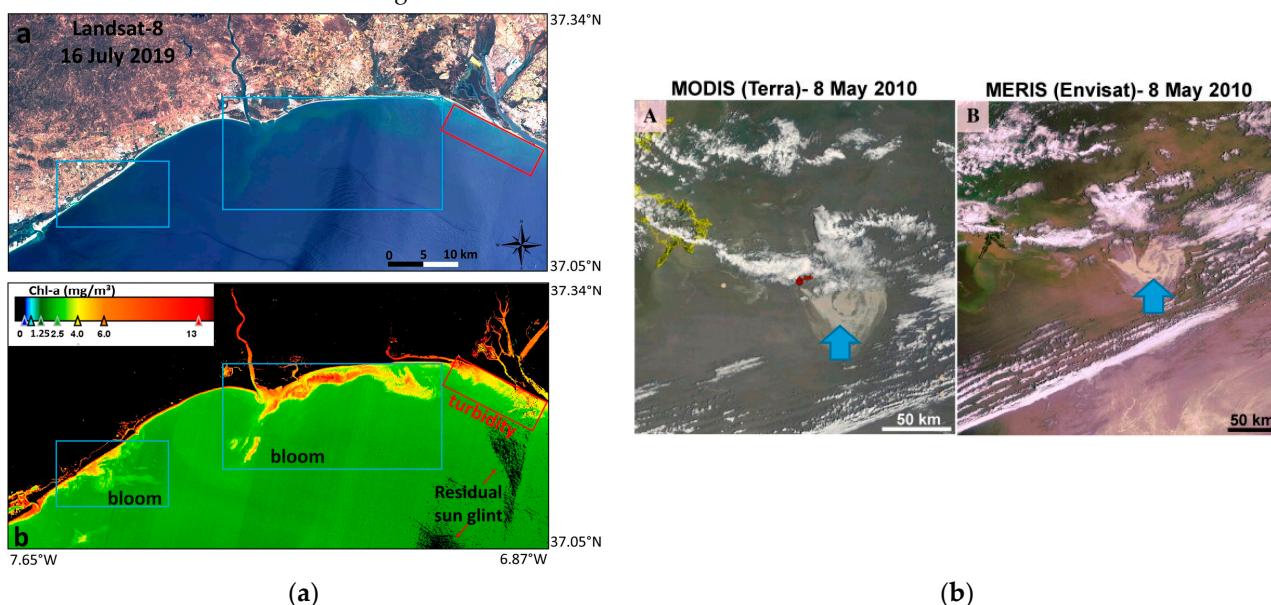


Figure 2. The polyedra algal bloom and oil spill of remote sensing images. (a) Landsat-8 RGB (bands 4-3-2) composite in this study region on 16 July 2019; (b) chl-a concentration (mg/m^3) after atmospheric correction with ACOLITE for the same scene [15]. (A) MODIS; (B) MERIS showing the site of the DWH oil spill in blue arrow [16].

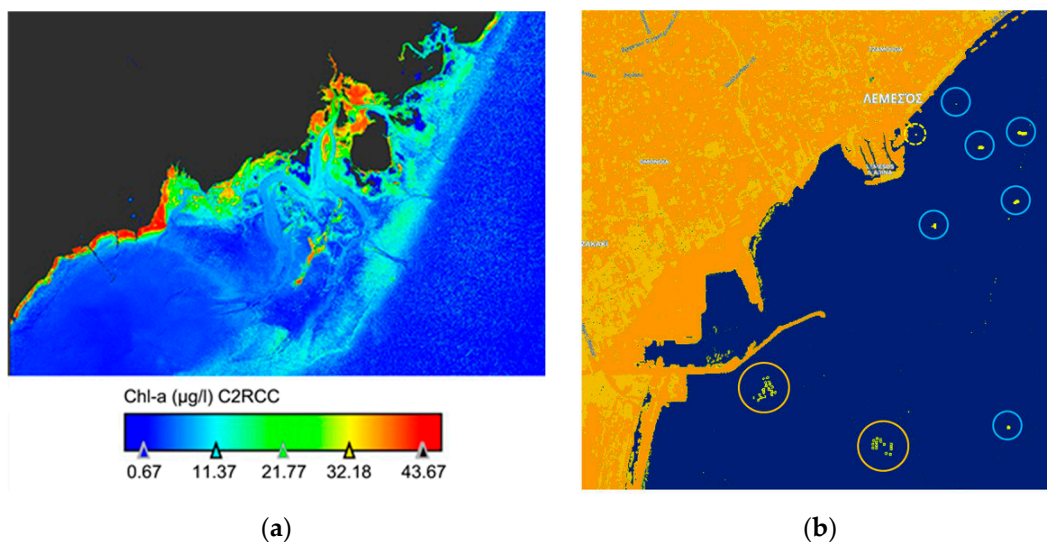


Figure 3. The LiDAR and MSI remote sensing images (a) show the spatial distribution of Chl-a (conc_chl) C2RCC in the Kneiss Archipelago, Gulf of Gabes, Tunisia [17]. (b) the floating plastic litter from space using Sentinel-2 imagery [18].

Previous studies have reviewed the literature in the remote sensing field from the perspective of satellite functions and monitoring targets; however, they have not adequately reviewed the field of marine pollution monitoring. Therefore, a global review of progress in remote sensing monitoring of marine pollution is needed, which reviews the application domains of marine remote sensing technology and the progress in marine pollution monitoring (Figure 4), serving as a reference for academic research and development efforts in using remote sensing technology for marine pollution monitoring.

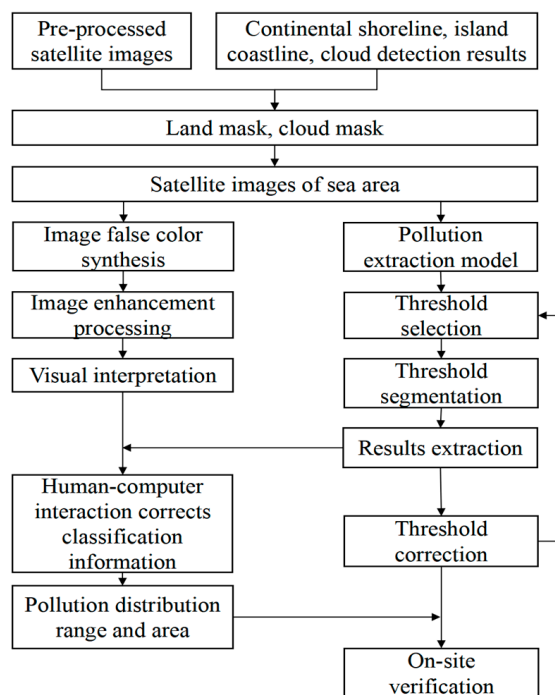


Figure 4. Framework of this study.

2. Sources and Monitoring Indices of Marine Pollution

The overexploitation of marine resources results in the degradation of the marine ecosystem and causes pollution, which damages the marine environment. The overexploitation, including major river conservation projects, land reclamation projects, coastal mining, offshore drilling, and mariculture, also leads to a shortage of marine resources and has negative impacts on coastal marine resources and environments. The utilization of marine resources varies in different regions due to differences in distribution, resulting in different types of pollution, such as land source, sea source and air source (Figure 5).

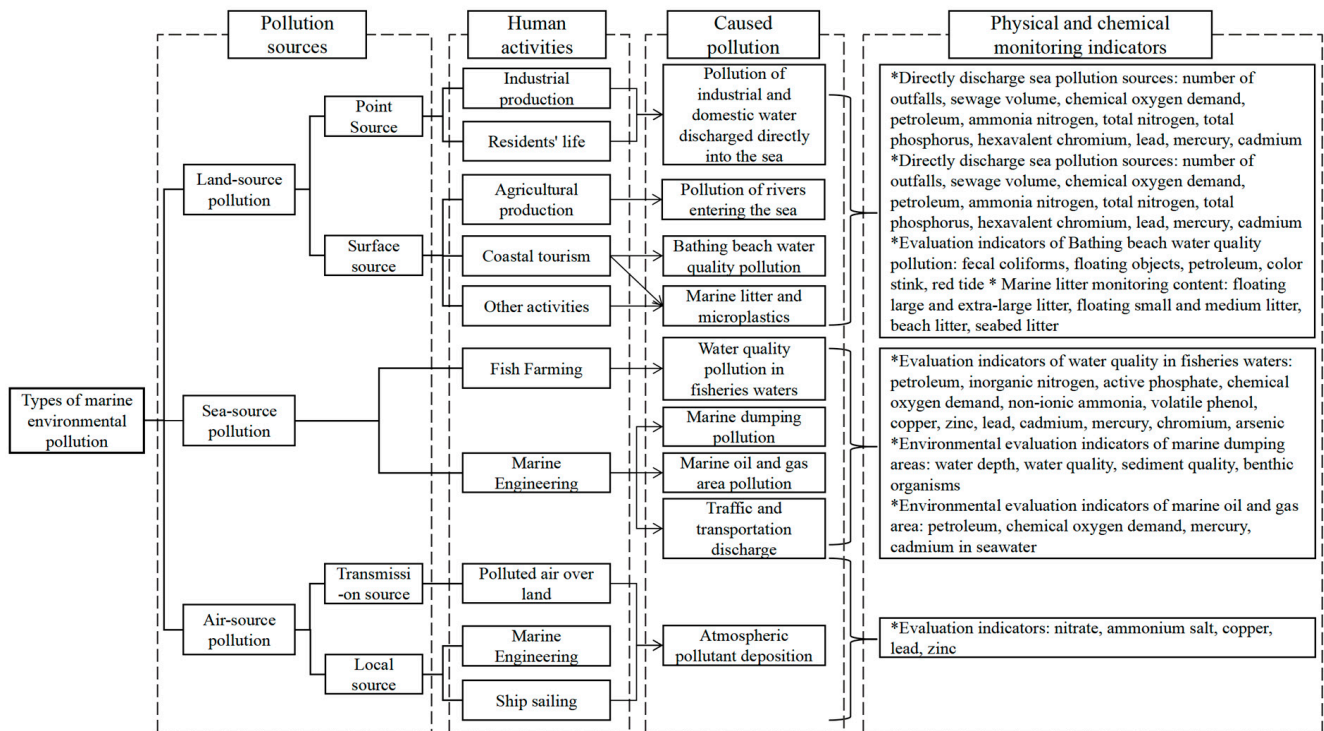


Figure 5. Source and monitoring index of marine pollution. Note: monitoring indices and methods from the Bulletin of China’s Marine Ecological Environment in 2020.

Land-source pollution has the widest distribution and largest quantity, accounting for 80% of the total marine pollution and having the most serious effect. Land-source pollution can be divided into two types: point-source and area-source. Point-source pollution is primarily composed of industrial waste water and domestic sewage that is collected and treated through sewage networks and discharged into the sea through designated discharge points [19,20]. Area-source pollution comes from agricultural runoff and livestock breeding activities, which flow into the ocean through runoff [20]. The root cause of land source pollution is human economic and social activity, which contributes to the negative impacts of such activities on the marine environment [21]. This type of pollution is not limited to coastal areas but is influenced by economic and social activities and is more pronounced in offshore regions with intensive secondary industries and rapid economic development [22]. Additionally, human activities on land can cause eutrophication and biotoxicity in sea areas through river dams and water storage projects and reduce river sediment discharge, leading to coastal erosion and changes in river water and groundwater quality [23,24]. Coastal tourism, being a popular form of tourism, also contributes to marine pollution through the construction of tourist resorts, docks, and breakwaters, which fragment coastal habitats and harm biodiversity, and through the pollution of seawater quality and the flow of beach litter into the ocean from bathing beaches [25]. The water quality of direct discharge into the sea is the main evaluation index for monitoring point-source land source pollution, while the water quality of seaport rivers, beach water, marine debris, and microplastics is the

main evaluation index for monitoring area-source land source pollution. Water quality is primarily evaluated according to the “Standard for Seawater Quality” (GB 3097-1997) [26], the “Standard for Surface Water Environmental Quality” (GB 3838-2002) [27] for rivers flowing into the ocean, and the “Guide for Monitoring and Evaluation of Bathing Beaches” (HY/T 0276-2019) for bathing beaches.

Sea-source pollution mainly refers to the pollution caused by human utilization of the sea. Marine pollution offshore is primarily caused by fishing and aquaculture practices. Overfishing has resulted in a reduction of fish resources, leading to the implementation of non-standard practices such as beach aquaculture, offshore cage aquaculture, and pelagic fishing, which negatively impact the marine environment by releasing nutrients and drugs into the water [28]. This can also pose a threat to coastal biodiversity, affecting beaches and mangroves [29]. Another significant source of marine pollution is marine engineering activities, such as oil and gas field exploitation, which can result in oil spills, sewage discharge, and seepage from eroded oil-bearing rocks. Additionally, the unregulated discharge of waste water from cruise ships and cargo ships in coastal tourism contributes to marine pollution [30]. Monitoring marine pollution includes monitoring the water quality of fishery waters and the discharge of waste water from marine engineering activities. The quality of fishery waters is evaluated according to the “Fishery Water Quality Standard” (GB 11607-1989) [31], while monitoring of marine engineering pollution in dumping areas and oil and gas fields should be based on the “Technical Regulations for Monitoring of Marine Dumping Areas” and “Technical Guidelines for Environmental Impact Assessment of Marine Engineering” (GB/T 17108-2006) [32].

Air-source pollution can be divided into transmission sources and local sources (Figure 6). Transmission sources refer to the pollution in the air that is transported from the land to the sea due to the influence of monsoons. Local sources refer to the pollutants that are emitted directly into the sea, such as oil and gas field exploitation, marine transportation, and fishing. The pollutants include SO₂, NO_x, CO, particulate matter, and VOCs. Atmospheric pollutants fall onto the marine surface through dry deposition and wet deposition processes [33]. Dry deposition involves the physical, chemical, and biological processes by which atmospheric pollutants fall onto the marine surface, while wet deposition involves ionic pollutants and soluble pollutants from the air falling onto the marine surface through precipitation or water vapor condensation [34]. The evaluation of marine atmospheric pollution deposition is mainly conducted based on the “Technical Regulations for the Assessment of the Flux of Atmospheric Pollutants Deposition into the Sea (Trial)” and includes the observation of the elements nitrate, NH₄Cl, Cu, Pb, and Zn.

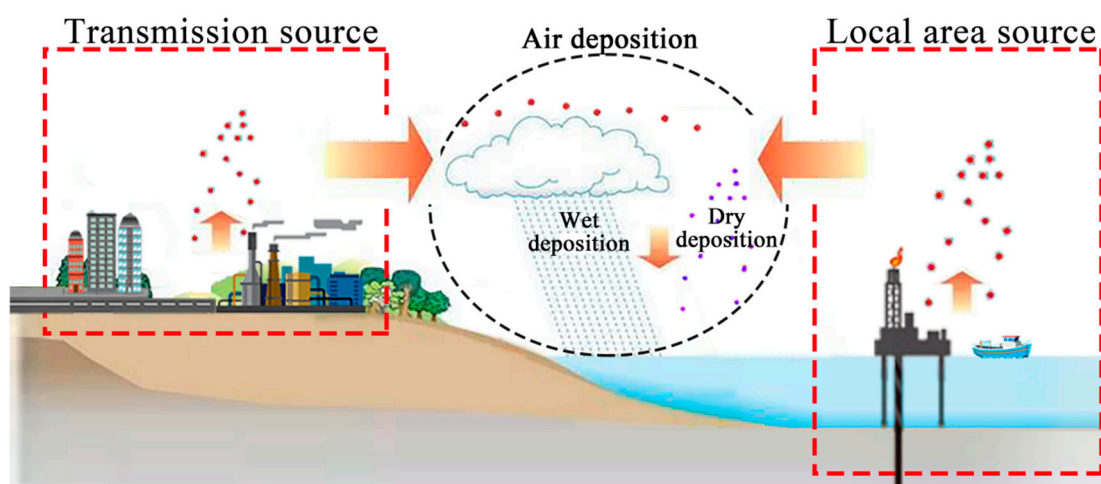


Figure 6. Mechanisms of marine atmospheric pollution transfer.

3. The Utilization of Remote Sensing Monitoring in Marine Pollution

3.1. An Overview of the Development History and Present Situation

In 1960, the United States launched the world's first meteorological satellite, TIROS-1, and used it to collect data on the marine surface temperature field from an altitude of approximately 700 km [35]. In 1978, the United States took the lead in the field of marine observation with the launch of Seasat-1, the first satellite dedicated to observing coastal seawater color [36], which marked the beginning of marine remote sensing monitoring. As the importance of marine resources continues to be recognized, more and more countries are investing in marine remote sensing technology to support monitoring efforts in the fields of shipping, environment, military, and economics [36–38].

The sensors commonly used in marine research include seawater color sensors, infrared sensors, microwave altimeters, microwave scatterometers, synthetic aperture radars, and microwave radiometers (Table 2). These sensors are capable of monitoring elements from the marine surface to the upper, lower, and bottom topography and can be used to monitor the seawater color and environment, as well as the marine dynamic environment (such as the marine surface wind field, marine surface height, effective wave height, and surface temperature) [39–41]. The sensors play a crucial role in monitoring islands, coastal zones, and other targets, including the marine wave field, storm surge floodplain, internal waves, sea ice, and oil spills. With the progress in microwave, infrared, and hyperspectral remote sensing technologies and their wider applications in the water, ecological, and air environments, the types of sensors available have become more diverse and specialized, and the spectral bands more refined. For example, China has launched a series of marine satellites, including HY-1C/D and HY-2B/C/D, equipped with new ultraviolet imagers, onboard calibration spectrometers, automatic ship identification systems (Figure 7), and other loads, providing a wealth of data for monitoring the global seawater color and dynamics [42]. The spectral bands of remote sensing images are getting finer and finer, forming multispectral, hyperspectral, and ultraspectral. At present, the spectral resolution in the 100 nm order is called multispectral, such as a remote sensor in the visible light and near-infrared spectral region only a few bands, such as the United States LandsatMSS, TM, SPOT in France, etc. The spectral resolution is in the 10 nm order, which is called HyPerspectral remote sensing. With the further improvement of the spectral resolution of remote sensing, remote sensing enters the ultraspectral stage when the spectral resolution reaches 1 nm. Hyperspectral and ultraspectral remote sensing are the frontier fields of remote sensing technology. It uses many very narrow electromagnetic wave bands to obtain relevant data from objects of interest so that substances that are not detectable in wide-band remote sensing can be detected. Chuanpeng Zhao et al. [43] proposed a new approach with solid improvements in dual-temporal image construction, misclassification processing, and tacit knowledge analysis, generated an accurate coastal salt marsh map at a national scale, and provided a classification mechanism for dual-temporal image-based coastal salt marsh identification and mapping. Remote sensing technology has huge advantages in obtaining real-time, large-scale, wide-area, and multi-period comparisons of basic coastal zone data. However, due to the indirect reflection of the characteristics of each observation object through the radiation and reflection characteristics of electromagnetic waves, the resolution is lower than that of conventional ground or ship observation methods. In addition, the presence of the phenomenon of homologous objects with different spectra and foreign objects with the same spectrum makes it difficult to recognize and interpret images.

Table 2. Satellite sensors information for marine research.

Sensor Type	Function	Representative Satellite Sensors	Satellite	Country/Region	Time	Spectral Band	Resolution	Revisit Cycle
Seawater color sensor	Monitoring of marine surface chlorophyll concentration, suspended mass concentration, marine primary productivity, diffuse attenuation coefficient, other marine optical parameters [44]	Coastal Zone Color Scanner	NIMBUS-7	United States	1978	5 visible near-infrared bands (0.443~0.750 μm), 1 thermal infrared band (11.5 μm)	0.825 km	1 day
		Sea-viewing Wide Field of View Sensor	SeaStar	United States	1997	8 bands (0.402~0.885 μm)	1.1 km (IFOV)	1 day
		Moderate-resolution Imaging Spectroradiometer	EOS-AM(TERRA)/EOS-PM(AQUA)	United States	1999/2002	36 discrete spectral bands (0.4~14.4 μm)	0.25~1 km	0.5/1 day
		Chinese Ocean Color and Temperature Scanner	HY-1A	China	2002	10-band (0.402~12.50 μm)	1.1 km	1 day
		Chinese Ocean Color and Temperature Scanner	HY-1C	China	2018	10-band (0.402~12.50 μm)	1.1 km	1 day
		Medium Resolution Spectral Imager	FY-3	China	2008	20-band (0.43~12.5 μm)	0.25~1.1 km	5.5 day
		Chinese Ocean Color and Temperature Scanner	HY-1D	China	2020	10-band (0.402~12.50 μm)	1.1 km	1 day
Infrared sensor	Measurement of marine surface temperature	Ocean Colour Monitor	OceanSat-3	India	2022	3 bands	360 m	2 days
		Advanced Very High Resolution Radiometer	NOAA/TIROS	United States	1979	2 thermal infrared channels (11 μm , 12 μm)	1.1 km (IFOV)	0.5/1 day
		Along-Track Scanning Radiometer	ERS-1/2	Europe	1991/1995	2 thermal infrared channels (11 μm , 12 μm)	1 km	3 days (TIR)/6 days (SWIR)
		Advanced Along-Track Scanning Radiometer	ENVISAT	Europe	2002	11/12 μm channel during daytime and 3.7/11/12 μm channel at night	1 km (IFOV)	3 days (TIR)/6 days (SWIR)
		VistA Integration Reporting and Revenue	FY-3A	China	2008	10 channels (including visible channels, 3 infrared atmospheric window channels)	1.1 km	5.5 days

Table 2. Cont.

Sensor Type	Function	Representative Satellite Sensors	Satellite	Country/Region	Time	Spectral Band	Resolution	Revisit Cycle
Microwave altimeter	Measurement of mean sea level height, geoid, effective wave height, marine surface wind speed, surface laminar flow, gravity anomalies, rainfall index	Radar altimeter	ERS-1/2	Europe	1991/1995	C-band/5.3 GHz	20 km (IFOV)	10 days/1 month
		Dual frequency radar altimeter, Single frequency altimeter	Jason-1	United States, France	2001	NRA: Ku-band/13.6 GHz and C-band/5.3 GHz; SSALT: Ku-band/13.65 GHz	25 km	10 days
		Radar altimeter-2	ENVISAT	Europe	2002	Ku-band/13.5 GHz	20 km (IFOV)	10 days/1 month 14 days in the early stage, 168 days in the late stage
		Radar altimeter	HY-2B	China	2018	Ku-band/13.58 GHz, C-band/5.25 GHz	2 km	
Microwave scatterometer	Measurement of the wind field at 10 m above sea level	Single-frame side-scan vertical transmit vertical receive (VV) radar	ERS1/2	Europe	1991/1995	C-band/5.3 GHz	Optimal: 50 km; Sampling: 25 km	3 days on average
		Double amplitude side scan scatterometer	ADEOS	Japan	1996	Ku-band/13.995 GHz	Optimal: 50 km; Sampling: 25 km	1.5 days
		Sea Winds scatterometer	QuikSCAT	United States	1999	Ku-band/13.4 GHz	Optimal: 50 km; Standard: 25 km; Sampling: 12.5 km	1 day
		Microwaves scatterometer	HY-2B	China	2018	Ku-band/13.256 GHz	25 km	14 days in the early stage, 168 days in the late stage
		Sector beam rotational scanning scatterometer	CFOSAT	China, France	2018	Ku-band/13.256 GHz	25/12.5 km	real time

Table 2. Cont.

Sensor Type	Function	Representative Satellite Sensors	Satellite	Country/Region	Time	Spectral Band	Resolution	Revisit Cycle
Synthetic aperture radar	Monitoring of wave direction spectrum, mesoscale eddy, ocean internal waves, shallow sea topography, marine surface pollution, marine surface characteristic information [45]	Active Microwave Instrument Synthetic Aperture Radar	ERS-1/2	Europe	1991/1995	L-band/1.275 GHz, S-band/3.0 GHz, C-band/5.3 GHz, X-band/9.6 GHz	30 m	1.5 month
		Ka-band Radar	SWOT	United States	2023	Ku band/C band	/	20.8 days
		Multi-polarized Advanced Synthetic Aperture Radar	ENVISAT-1	Europe	2002	C-band/5.3 GHz	30 m~1 km	5 days/3 months
		Multi-polarized C-band synthetic aperture radar	GF-3	China	2016	C-band/	1 m (highest)	1 week
		Line Leveling Passive Microwave Radiometer	RCM-3	Canada	2019	C-band/5.405 GHz	1 m (highest)	12 days
Microwave radiometer	Measurement of marine surface temperature, marine surface wind speed, sea ice water vapor content, CO ₂ and sea-air exchange	Line Leveling Passive Microwave Radiometer	DMSP	United States	1987	4 bands (19.35, 2.235, 37.0, 85.5 GHz) 7 channels	61 × 66 cm antenna diameter	1 day
		Microwave Scanning Radiometer	MOS-1	Japan	1987	2 bands (23.8 GHz, 31.4 GHz)	23 km	5 days
		Multi-frequency scanning microwave radiometer	Seasat-A/Nimbus-7	United States	1978	5 bands 9 channels	(31.4 GHz) /32 km	2 days
		Advanced Microwave Scanning Radiometer -E	EOS-PM(AQUA)	Europe	2002	6 bands 12 channels	(23.8 GHz) /22~120 km	1 day
		Advanced Microwave Scanning Radiometer	ADEOS-2	Japan	2002	8 bands 14 channels	(37~6.6 GHz) Antenna diameter 1.6 m	1 day
		Scanning Microwave Radiometer Imager MWRI	HY-2B	China	2018	5 bands (6.925, 10.7, 18.7, 23.8, 37.0 GHz)	Antenna diameter 2 m	14 days in the early stage, 168 days in the late stage
		Calibration Microwave Radiometer	HY-2D	China	2021	6 bands (3.58, 5.25, 13.256, 18.7, 23.8, 37 GHz)	Antenna diameter 1.2 m	10 days
Poseidon-4 radar altimeter and microwave radiometer	Sentinel-6	United States, Europe	2020	C-band/Ku-band	/	10 days		



Figure 7. Image observed by PALSAR-2, synthetic aperture radar onboard ALOS-2, at 10:23 (UTC) on March 26 (a) around the Suez Canal; (b) extended image around the stranded ship (Picture source: Earth Observation Research Center).

3.2. The Monitoring Data and Methods

Marine remote sensing has the unique advantages of all-weather, wide-range, and long-term observation and is widely used in marine ecology and resources monitoring, marine disaster monitoring, marine rights and interests maintenance, marine environmental prediction and security assurance, and other fields. Therefore, marine pollution can be monitored and reversed based on marine remote sensing data. Marine pollution monitoring can be classified into three aspects: seawater quality, marine debris and microplastic pollution, and atmospheric deposition pollution. According to the application focus of remote sensing, the remote sensing data products and research methods for monitoring the pollution of these marine areas are analyzed.

3.2.1. Seawater Quality Monitoring

Marine remote sensing is widely used in a variety of fields, including marine ecology and resource monitoring and marine disaster monitoring [46]. With the help of remote sensing, it is possible to reverse and monitor marine pollution. The main environmental indices monitored by remote sensing include the suspended solids content, chlorophyll-a concentration [47], colored soluble organic matter, and other comprehensive pollution indices [46,48]. To invert the quality of water environmental indices, a spectral model must be established and combined with monitoring data. Remote sensing inversion is often performed using visible light bands (Table 3), and various methods such as empirical models, theoretical models, semi-analytic models, and others can be used (Table 4). The suspended solids content in water can be reversed by fitting a formula that correlates the measured suspended solids content with remote sensing reflectance or turbidity [49–51]. The concentration of chlorophyll-a is a direct indices of eutrophication and organic pollution, and the inversion methods of chlorophyll-a concentration include chlorophyll fluorescence, band models, nonlinear mapping, and mechanism model methods [52–54]. Chromophoric soluble organic matter is another important component of dissolved organic matter that can be monitored remotely through the development of a remote sensing inversion model [55–57]. For example, red tides have posed a huge threat to the resources and environment of coastal areas. Multi-spectral scanners can be used to monitor red tides, whose visible/infrared multispectral radiometers can provide information on the location, range, water color type, changes in phosphate concentration on the sea surface, and the direction of red tide diffusion and drift to take timely measures to control them [58].

It is difficult to find independent spectral characteristics in seawater quality indices, such as dissolved organic carbon, water temperature [59], transparency, dissolved oxygen, chemical oxygen demand, five-day biochemical oxygen demand, total nitrogen, total phosphorus, etc. As a result, indirect remote sensing analysis must rely on the correlation between different substances [60–62]. However, remote sensing monitoring also has limitations, such as difficulty in estimating pollutants in the vertical dimension of water bodies and the limitation of partial inversion to estimate only general parameters, not specific types of marine pollution. Coastal human activities and the complex dynamic environment of the sea can also affect the water quality, requiring higher performance from satellite sensors to monitor it effectively through remote sensing technology [63]. Despite the progress in remote sensing technology, the main drawback of physical-chemical sensor systems is their lack of specificity and sensitivity and their inability to assess the environmental concentration of most marine pollutants. In this regard, biosensors may offer the required specificity and selectivity [64].

Table 3. The monitoring data for seawater quality.

Seawater Quality Indices		Data
Suspended solids content	Remote sensing data	Sentinel-3A OLCI [65], SPOT, Terra ASTER, Landsat TM/ETM, Envisat MERIS [66], COMS GOCI [67–69]
	Measured data	Seawater sampling data, official water environment monitoring samples, measured spectral data Non-space remote sensing data: AVIRIS, CASI, OMIS, AISA, etc.;
Chlorophyll-a concentration	Remote sensing data	Remote sensing data: Envisat MERIS, CBERS-2 CCD, Terra/Aqua MODIS [70,71], EO-1 Hyperion, Terra ASTER, Landsat MSS/ETM+, HJ-1 CCD, et al.
	Measured data	Ground-measured spectral data: ASD, GER, etc.
chromophoric dissolvable organic matter	Remote sensing data	Sentinel-2 [72], Landsat 8 OLI, SeaWiFS, Aqua/Terra MODIS [73], etc.
	Measured data	Water sampling data

Table 4. The monitoring methods for seawater quality.

Methods	Characteristics
Empirical models (single band model, band ratio model, multiple regression model, nonlinear model, machine learning)	Based on the relationship between water spectral information and measured water quality parameters, the algorithm is relatively mature and the process is simple, but it lacks physical basis
Theoretical model	The combination of water quality spectral characteristics and statistical analysis has a certain physical basis, but for the model requiring higher precision, the process is more complicated and the universality is poor
Semi-analytical model	Based on the relationship between apparent optical quantity and measured water quality parameters, it has a strong physical mechanism and good universality, despite the difficulty of model establishment [72]

The quality of seawater can be negatively impacted by large-scale pollutants such as red tides, green tides, and oil spills, especially due to increased human activities leading to increased inputs of nitrogen and phosphorus in the ecosystem (Table 5) [74–77]. Remote sensing technology plays a crucial role in monitoring such events by monitoring the seawater quality indices over large areas [78,79]. The research has shown that the multi-band

ratio method can be used to monitor floating algae and reduce interpretation errors [80–82]. Several algorithms have been proposed, including the Floating Algae Index (FAI) [83,84], the Normalized Algae Index (NDAI) [85], the Virtual Baseline Index of Floating Algae Height (VB-FAH) [86], and the Multi-Spectral Green Tide Index (MGTI) [87,88]. However, these algorithms require complex and accurate atmospheric correction procedures, which can increase the complexity of interpretation. To address this, Zhang Hailong et al. developed the Floating Algae Index (FGTI) based on the DN values of different satellite data, and Chen Ying et al. [89] proposed the Green Tide Index (TCT-GTI) algorithm based on the Tassel Cap Transformation method, which requires no atmospheric correction.

Table 5. The Monitoring data and methods for marine green tide pollution disaster.

Author	Time	Satellite/Sensor	Waveband Range	Algorithm	Characteristics
Hu [78]	2009	Aqua/Terra MODIS	V, NIR, SWIR	Floating Algal Index	It is less sensitive to changes in environment and observational conditions (aerosol type and thickness, sun/observational geometry, and solar brilliance) and can penetrate thin clouds, providing a simple and effective means of atmospheric correction and making it easier to establish image-independent thresholds to monitor and quantify planktonic macroalgae.
Shi et al. [85]	2009	Aqua/Terra MODIS	SWIR	Normalized Algae Index	The effect of atmospheric molecular scattering is removed, making the NDAI more sensitive to the radiance signal from the marine surface [85].
Son [90]	2012	GOCI	V, NIR	GOCI floating green tide index	The muted or subtle signal of planktonic green algae is enhanced and separated from the surrounding complex water signal [90].
Xing et al. [86]	2016	HJ-1A/1B	V, NIR	Virtual Baseline Index of Floating Algal Height	Even without the use of the shortwave infrared (SWIR) band, VB-FAH appears to be comparable to the planktonic algal index (FAI).
Zhang et al. [88]	2016	GF1 WFV, HJ CCD	V	Multispectral Green Tide Index	It can effectively eliminate the influence of external interference, such as suspended sediment and thin clouds, and has low sensitivity to the environment [88].
Zhang et al. [91]	2019	GF-1 WFV1, GF-1 WFV3, HJ-1B CCD, Landsat-7 ETM+, GOCI	V, NIR, SWIR	Floating algae index	The use of tasseled cap transformation is more powerful than traditional NDVI (normalized vegetation index) in responding to perturbations from environmental conditions, observational geometry, sunlight, and thin cloud pollution [88,91].
Chen et al. [89]	2020	GOCI	V	Green Tide Index	No atmospheric correction is required [89].

Monitoring red tides can be conducted by using the spectral and temperature characteristics of the affected water bodies and through the analysis of optical satellite data (Table 6). The main methods of red tide remote sensing monitoring include the Chlorophyll Concentration Anomaly Method, the Red Tide Index (MRI), the Rrs Band Ratio Method, the Red Band Difference (RBD), the RBD_KBBI (*Karenia brevis* Bloom Index), and others [92,93]. Jiang Dejuan et al. [92] emphasized that the effectiveness of red tide monitoring is dependent on the type of sensor, algorithm, and remote sensing time. Therefore, it is

necessary to combine field survey data or ERGB images with the remote sensing data to verify the accuracy of red tide monitoring in different times and regions [94,95].

Table 6. The monitoring methods for the marine red tide pollution disaster.

Research Methods	Characteristics
Chlorophyll concentration anomaly method	It characterizes the most important characteristic parameters of red tide but is usually overestimated.
Red tide index	It can enhance the difference between the red tide water body and the surrounding water body; therefore, it can be used for the determination of red tide.
Band ratio method	Using the ratio of reflection and absorption bands of red tide water bodies, we can extract red tide information.
Red band difference method	The method is based on the high fluorescence property of dinoflagellate water bloom.
RBD_ KBBI	The red tide monitoring index proposed is based on RBD.

Note: Compiled from references [92].

Marine engineering encompasses a variety of activities, including marine dumping, marine oil and gas transportation, and others. The main source of seawater quality and environmental degradation in the ocean is oil spills caused by ships during berthing at ports, navigation, and accidents [96,97]. Early monitoring, tracking, and diffusion of oil spills is crucial in designing effective algorithms for remote sensing monitoring [98]. However, the current methods for oil spill monitoring often overlook the space-time characteristics and laws of the interaction between oil spills and the ocean [99]. Different remote sensing technologies, such as microwave radar, optical (multi/hyperspectral remote sensing), thermal infrared, and others, can be used to monitor marine oil spills. Microwave radar remote sensing is one of the main methods and is based on the different absorption and transmission properties of water and oil in electromagnetic waves. This method is mainly used to extract the oil spill extent by identifying the “dark pixel” feature in the microwave radar image [100,101]. Spectral response characteristics of oil spill simulation experiments can be used to identify, classify, and quantify the types of oil spills [102,103]. Optical remote sensing can also be used for the identification and classification of oil spills [104–106]. Solar reflected light can be used to monitor the oil spill thickness on the marine surface; however, the monitoring range is limited to less than 0.4 mm due to the different absorption, scattering, and reflection effects of oil spills on incident light. Thermal infrared remote sensing has a larger monitoring range; however, the ability to monitor oil spills is weaker than that of optical remote sensing due to the differences in existing spaceborne sensors [107]. In a study of oil spills caused by marine accidents, Lu Yingcheng et al. [105] used a GF-3 SAR image to delineate “suspected oil spills” and analyzed the optical anomalies of the “Sanji” oil spill incident in the East China Sea in 2018 using Sentinel-2 multi-spectral remote sensing data (MSI) from the European Space Agency. This study resulted in the optical remote sensing identification and classification of different types of oil spills. Huang Ke et al. [104] used GF-1 satellite data along with a thin oil film thickness model to calculate the oil film thickness of the oil spill area and estimate the oil spill caused by the explosion of the Huangwei oil pipeline in Qingdao in 2013. Remote sensing monitoring of oil spills at sea is influenced by marine environmental conditions, such as marine surface wind speed, and therefore, a combination of sea wave spectrum and wind wave information is necessary for further research [108,109].

3.2.2. Debris and Microplastics Monitoring

Marine debris and microplastics have a significant negative impact on marine organisms, ecosystems, fisheries, and tourism [110,111]. The monitoring of these pollutants in the ocean through remote sensing can be effectively accomplished by using sensitivity analysis, optical simulation, and satellite image spectral analysis (Table 7) [112,113]. The reflection spectra of known marine floating objects can be utilized for this purpose [110,114]. Most

of the research and monitoring of marine debris is focused on plastic waste and utilizes optical sensors operating in the visible light, near-infrared, and short-wave infrared spectral ranges, as well as SAR sensors and other image data sources [115]. However, microplastics are plastic pollutants with a diameter of less than 5 mm and cannot be effectively identified through satellite images due to their small size. While there have been efforts to observe microplastics in water, through optical means such as lasers and polarization, there is still a significant gap in terms of satellite observation. SAR sensors are commonly used to monitor marine debris and microplastics by identifying surface active agents on the marine surface. The classification methods for marine debris monitoring are mainly manual classification, use of indices, spectral classification, or machine learning [115]. The use of unmanned aerial vehicles and artificial intelligence for monitoring beach litter is an emerging field [116]. Machine learning has been shown to significantly increase the speed of screening for marine debris, operating 39 times faster than human screening in cases of low sensitivity [116]. The development of a spectral characteristic model for marine debris or microplastics is also an area of exploration. Goddijn-Murphy et al. proposed a reflection model based on geometric optics and the spectral characteristics of plastics and seawater to describe the interaction between sunlight and floating microplastics on the marine surface.

The use of satellite data are useful tool in monitoring marine debris as it can provide repeated global coverage data at various scales and resolutions, which is not possible through field observations or remote sensing with ships, aircraft, or unmanned aerial vehicles. However, the limitations of optical satellite data include limited temporal coverage due to fixed time and factors such as the sun, clouds, atmospheric aerosols, sensor saturation on surfaces such as ice, sand, or snow, and a high solar zenith angle. Additionally, the spatial resolution of satellite data are typically greater than 1 m, making it difficult to monitor marine debris smaller than this resolution [117]. For the limitation, it is possible to solve this problem by improving the accuracy of remote sensing observation instruments. Furthermore, through multi-band remote sensing observation methods, we can gain a deeper understanding of the electromagnetic wave characteristics of ground objects and separate information from different observation objects.

Table 7. Remote sensing monitoring data and methods for marine debris and microplastics.

Author	Time	Band Range	Satellite/Sensor	Types of Plastic Waste	Monitoring Methods	Classification Methods
Hamilton [117]	2015	MW	RADARSAT-2	Marine surface float (marine bacteria associated with surfactants)	Observe oil slicks to monitor marine surface slicks using the association among bacteria produced by surfactants and oil slicks (Hamilton et al., 2015)	Machine learning techniques
Aoyama [118]	2016	NIR/SWIR	Worldview-2	Marine debris	Find common spectral features associated with the presence of plastic [118]	Spectral classification method
	2016	NIR/SWIR	Worldview-3	Buoys around fishing nets	Propose the spectral angle mapper (SAM) classification method [118]	Spectral classification method
Kurata [119]	2016	MW	RADARSAT-2	Marine surface float (marine bacteria associated with surfactants)	Observe oil slicks to monitor marine surface slicks using the association among bacteria produced by surfactants and oil slicks [119]	Machine learning techniques
Davaasuren [120]	2018	MW	Sentinel-1A, COSMO-SkyMed	Microplastics (surfactants, sea mud and biofilms)	Observe oil slicks to monitor marine surface slicks using the association between bacteria produced by surfactants and oil slicks [120]	Machine learning techniques
Goddijn-Murphy	2018	V~SWIR	--	Floating microplastics	Model the reflection of sunlight interacting with the marine surface of floating microplastics	Model building
Howe [121]	2018	MW	TerraSAR-X	Marine surface float (marine bacteria associated with surfactants)	Observe oil slicks to monitor marine surface slicks using the association between bacteria produced by surfactants and oil slicks [121]	Machine learning techniques
Topouzelis [115]	2019	V, NIR	Sentinel-2A	Artificial floating plastics (water bottles, LDPE plastic bags and nylon fishing nets)	Supervised classification [108]	Machine learning techniques
	2019	MW	Sentinel-1			
Biermann	2020	V, NIR, SWIR	Sentinel-2 MSI	Piece of floating large plastic	Develop novel float index (FDI) algorithms to monitor floating plastics and distinguish them from natural floats	Usage index
		V, NIR	Planet P			
Kikaki [111]	2020	NIR, SWIR	Sentinel-2 MSI	Floating plastic debris	Monitor and validate floating plastic debris by systematically recording and assessing the spectral characteristics of pure floating plastic and distinguishing it from other floating materials on the marine surface (e.g., Sargassum, foam)	Manual classification
		NIR, SWIR	Landsat-8 OLI			

3.2.3. Inversion of Atmospheric Pollution Deposition

The monitoring of atmospheric pollution deposition typically involves measured data, model simulations, and remote sensing. Atmospheric pollution deposition in the ocean can be classified into three sub-categories that are influenced by the distribution of aerosols: clean ocean, marine minerals, and marine pollution [122]. Therefore, the monitoring of atmospheric pollution deposition can be conducted through aerosols. Remote sensing by satellite is a highly effective research method for observing the global distribution of aerosols, their optical properties, and their radiation effects due to the large spatial and temporal variations of aerosol distribution [123]. Aerosol optical thickness, a key parameter of aerosols, characterizes atmospheric turbidity and is a critical factor in determining the impact of aerosols on climate [124,125]. Some of the satellite sensors used to monitor atmospheric pollution deposition include the Global Ozone Monitoring Experiment (GOME), the Atmospheric Mapping Scanning Imaging Absorption Spectrometer (SCIAMACHY), the Ozone Monitor (Aura OMI), the Interferometric Infrared Atmospheric Detector (METOP/IASI), the FY-3 Total Ozone Detector (FY-3 TOU), and the UV Ozone Vertical Detector (FY-3 SBUS) of FY-3 [126,127].

Remote sensing monitoring calculates the concentration of deposition according to the formula by reversing the density of the vertical gas column, and then calculates the dry and wet deposition flux in combination with the dry and wet deposition calculation formula. For example, Dong Haiying et al. [124] used Terra MODIS data to reverse the 10 km resolution aerosol optical thickness and analyzed that the aerosol concentration gradually decreased from the coastal waters to the outer sea due to the influence of land-based pollution components, and there was a high aerosol optical thickness in the coastal Bohai Sea, the Yellow Sea coast, and the Yangtze River estuary. SeaWiFS aerosol optical thickness products can be used to study aerosol distribution and change characteristics. Hao Zengzhou et al. [128] analyzed the aerosol distribution in China's sea area and found that the average aerosol optical thickness in the eastern China sea area has a zonal distribution centered on the middle latitude and has seasonal changes. From spring to winter, the aerosol optical thickness shifts from the high latitude sea area to the low latitude sea area, and the scope is also gradually expanding. Mao Ying [122] over the sea air will be visible infrared imaging radiometer VIIRS, medium resolution imaging spectrometer MODIS, stationary seawater color satellite imager GOCI, and geosynchronous meteorological satellite AHI H8 aerosol optical thickness product data combined with field measured data. Compared with other aerosol optical thickness remote sensing products, GOCI aerosol optical thickness products show the characteristics of high sampling frequency and high precision.

The inversion results of aerosol optical thickness remote sensing products are affected by a variety of factors, including the signal-to-noise ratio of the sensor itself, the accuracy of the calculation of the surface reflectance of the underlying surface, and the rationality of the selection of the preset aerosol model [122]. At the same time, the frequent human activities and pollutant emission and diffusion, as well as the unique physical geography and hydrological conditions of the sea area, will cause the sea area reflectivity to include many factors, not only the atmospheric impact but also the role of the seawater itself, which is more obvious in the coastal sea area.

4. Conclusions and Future Prospects

4.1. Conclusions

This paper summarizes the progress in the application of remote sensing for marine pollution monitoring. Coastal areas are subjected to various forms of pollution from land, sea, and air sources due to the difference in urbanization and industrialization, leading to a degradation in the quality of the marine environment and having significant impacts on marine ecology. Remote sensing monitoring of marine pollution encompasses various aspects, including seawater quality, marine debris and microplastic pollution, and the inversion of atmospheric pollution depositions. With the launch of various marine monitoring satellites, remote sensing provides a wealth of data sources to monitor marine hydrology

and environmental parameters. Remote sensing can provide information on environmental parameters and habitats and monitor human activities, thus improving the marine environment to some extent (Figure 8). Monitoring seawater quality and temperature mainly uses remote sensing of seawater color and temperature, which is effective in monitoring seawater quality deterioration and large-scale coastal seawater quality changes during disasters. The methods of monitoring marine debris and microplastics have evolved from remote sensing inversion to machine learning. The research into remote sensing monitoring of marine atmospheric pollution deposition, which only quantifies atmospheric pollution through aerosol thickness, is inadequate. It is crucial to integrate measured data, remote sensing monitoring, and information services to achieve comprehensive monitoring and assessment of marine pollution. Moreover, there are a number of marine remote sensing products worldwide; however, there are significant differences in accuracy and other aspects of similar products in different countries, leading to technical barriers that pose challenges to marine governance decisions and environmental protection in various countries and regions. Therefore, developing three-dimensional monitoring techniques, combining different types of sensors, and establishing a comprehensive marine monitoring database is of great significance, along with data, technology, and standard sharing, to monitor the marine environment and realize the sustainable development of marine resources.

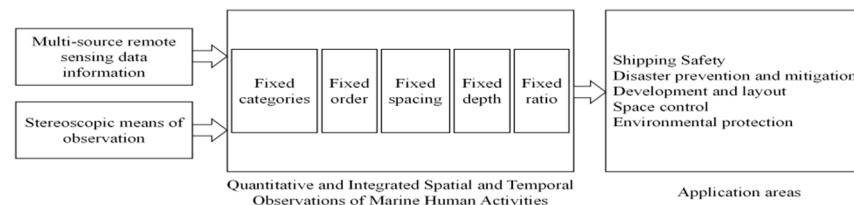


Figure 8. The extraction process of marine pollution data. Note: Redraw from reference [8].

4.2. Future Prospects

4.2.1. The Tendency of Three-Dimension in Marine Monitoring

Despite its practicality, remote sensing monitoring has limitations in its ability to identify and quantify the majority of marine pollutants. Due to the complex three-dimensional nature of the ocean, most remote sensing methods can only obtain information from the upper layer, with the exception of the altimeter used for rough sounding. The best conditions for optical sensors to penetrate the seawater surface are up to 27 m, while air sensors can only reach up to 46 m [129,130]. This resolution limitation of the image data affects the vertical dimension of marine pollution monitoring and assessment and cannot provide a quantitative method for tracing the levels of individual substances. Thus, the development of remote sensing technology that can monitor deep-sea pollution is a crucial goal for the future [117,131]. Although monitoring the deep sea may monitor less pollution than the upper sea, three-dimensional marine observation remains the key direction for the progress of remote sensing technology. Furthermore, multi-source data integration with three-dimensional ocean numerical models for marine pollution monitoring should be used. Observations obtained through remote sensing and sensors are not sufficient to project the 3D structure of the marine environment. Hence, 3D hydrodynamic and ocean circulation modeling should be developed.

4.2.2. The Tendency of Multi-Source Data Fusion in Marine Pollution Monitoring

Despite the progress in remote sensing technology and the increasing availability of data, the accuracy of remote sensing data products can still be impacted by environmental factors such as spatial-temporal variability in the sky and on earth. The diversity of human activities in the ocean also limits the validity of remote sensing data for marine pollution monitoring. Currently, marine pollution monitoring primarily relies on field observations, utilizing biochemical indices, rather than solely relying on remote sensing. To improve the accuracy and reliability of marine pollution monitoring, it is necessary to integrate remote

sensing with other monitoring tools, such as ship sensors, buoy sensors, aircraft sensors, and marine ecological reserves/biosensor networks.

Remote sensing technology, such as high-resolution imaging, multi-spectral and hyper-spectral, fluorescence, and Raman molecular spectroscopy, can be used to measure different types of pollution; however, it is still not enough to replace on-site observations. For example, the movement of pollutants in the ocean is influenced by complex hydrodynamics and marine circulation, making it difficult for remote sensing technology to accurately track the diffusion of marine pollution. Additionally, micropollution may not cause large-scale pollution, and it is challenging to quantify using remote sensing alone.

Therefore, multi-platform and multi-means integrated observation technology is necessary for accurate marine environmental monitoring. This includes the establishment of a marine remote sensing database, which integrates satellite, aviation, ship, and shore-based data to provide a comprehensive monitoring system for marine environmental monitoring. The development of technology for collecting, storing, processing, analyzing, and utilizing multi-source data will be crucial for the progress of marine remote sensing. By providing timely information to the government and relevant entities, this database can support disaster prevention, mitigation, and the launch of emergency plans.

In addition, the importance of ground measurements and alternative satellite calibration systems (e.g., MOBY, AERONET, and GOOS) cannot be overlooked. The Marine Optical Buoy (MOBY), a radiometric buoy stationed in the waters off Lanai, Hawaii, has been the primary basis for the on-orbit vicarious calibrations of all three US ocean color sensors and numerous international satellite sensors since late 1996 [132]. The aErosol rObotic NETwork (AERONET) program is a federation of ground-based remote sensing aerosol networks established by NASA and PHOTONS. For more than 25 years, the project has provided a long-term, continuous, and readily accessible public domain database of aerosol optical, microphysical, and radiative properties for aerosol research and characterization, validation of satellite retrievals, and synergism with other databases. The Global Ocean Observing System (GOOS) consists of a variety of observation means and is committed to obtaining and disseminating reliable assessment and forecasting information on the present and future state of the marine environment for the effective, safe, and sustainable use of the marine environment.

4.2.3. The Benefit for the Sustainable Utilization of Marine Resources

The relationship between marine resources and the environment determines the sustainable utilization of the ocean, and remote sensing technology for monitoring marine resources and the environment can enable the effective implementation of marine spatial planning. In the governance of marine resources, remote sensing methods are used to strengthen the survey of the reserves and distribution of various marine resources and monitor the impact of human activities on marine development and environmental pollution. Based on the principle of unified coordination of economic, social, and ecological benefits, by studying the intensity and methods of human utilization of the ocean, we improve marine spatial planning, ensure the rational use of marine resources, and promote sustainable development of the marine economy. In addition, comprehensive monitoring data based on remote sensing databases is also the decision-making basis for marine scientific utilization.

Author Contributions: Conceptualization, J.M. and R.M.; methodology, Q.P. and X.L.; software, Q.P. and J.W.; validation, Q.P. and X.N.; formal analysis, J.M. and X.L.; investigation, Q.P. and J.W.; resources, R.M.; visualization, Q.P. and X.L.; supervision, R.M.; funding acquisition, J.M. All authors have read and agreed to the published version of the manuscript.

Funding: This research was supported by Key Laboratory of Ocean Space Resource Management Technology, MNR (Grant No. KF-2023-103), the Natural Science Foundation of Zhejiang Province, China [Grant No. LGF22D010002], the Open Funding of Zhejiang Collaborative Innovation Center

for Land and Marine Spatial Utilization and Governance Research [Grant No. LHGTX-2023-003], and Ningbo University Donghai Academy [Grant No. DH202302CBZZ03].

Data Availability Statement: Not applicable.

Conflicts of Interest: The authors declare no conflict of interest.

References

1. Sankar, T.K.; Kumar, A.; Mahto, D.K.; Das, K.C.; Narayan, P.; Fukate, M.; Awachat, P.; Padghan, D.; Mohammad, F.; Al-Lohedan, H.A.; et al. The Health Risk and Source Assessment of Polycyclic Aromatic Hydrocarbons (PAHs) in the Soil of Industrial Cities in India. *Toxics* **2023**, *11*, 515. [[CrossRef](#)] [[PubMed](#)]
2. Meshram, S.G.; Kahya, E.; Meshram, C.; Ghorbani, M.A.; Ambade, B.; Mirabbasi, R. Long-term temperature trend analysis associated with agriculture crops. *Theor. Appl. Clim.* **2020**, *140*, 1139–1159. [[CrossRef](#)]
3. Henrique, M.P.; Paul, W.L.; Vânia, P.; Rob, A.; Jörn, P.W.S.; Juan, J.F.M.; Araújo, M.B.; Patricia, B.; Reinette, B.; William, W.L.C.; et al. Scenarios for global biodiversity in the 21st century. *Science* **2010**, *330*, 1496–1501.
4. Ma, R.F.; Dou, S.M.; Gong, H.B. *China's East China Sea Sustainable Development Study: A Volume on Cross-Regional Governance of Coastal Zone Ecology and Environment*; Ocean Press: Beijing, China, 2019.
5. Sala, E.; Knowlton, N. Global Marine Biodiversity Trends. *Annu. Rev. Environ. Resour.* **2006**, *31*, 93–122. [[CrossRef](#)]
6. Lin, M.S.; Zhang, Y.G.; Yuan, X.Z. The development course and trend of ocean remote sensing satellite. *Acta Oceanol. Sin.* **2015**, *37*, 1–10.
7. Sun, F.Z. *Remote Sensing Assessment of Coastal Zones*; Science Press: Beijing, China, 2015.
8. Zou, B.; Lin, M.S.; Shi, L.J.; Zou, Y.R.; Jia, Y.J.; Zeng, T. Application of Remote Sensing Technology in Ocean Disaster. *City Disaster Reduct.* **2018**, *123*, 61–65.
9. Eck, T.F.; Holben, B.N.; Kim, J.; Beyersdorf, A.J.; Choi, M.; Lee, S.; Koo, J.-H.; Giles, D.M.; Schafer, J.S.; Sinyuk, A.; et al. Influence of cloud, fog, and high relative humidity during pollution transport events in South Korea: Aerosol properties and PM_{2.5} variability. *Atmos. Environ.* **2020**, *232*, 117530.
10. Fichot, C.G.; Tzortziou, M.; Mannino, A. Remote sensing of dissolved organic carbon (DOC) stocks, fluxes and transformations along the land-ocean aquatic continuum: Advances, challenges, and opportunities. *Earth-Sci. Rev.* **2023**, *242*, 104446. [[CrossRef](#)]
11. Leifer, I.; Lehr, W.J.; Simecek-Beatty, D.; Bradley, E.; Clark, R.; Dennison, P.; Hu, Y.; Matheson, S.; Jones, C.E.; Holt, B.; et al. State of the art satellite and airborne marine oil spill remote sensing: Application to the BP Deepwater Horizon oil spill. *Remote Sens. Environ.* **2012**, *124*, 185–209. [[CrossRef](#)]
12. Mace, T.H. At-sea detection of marine debris: Overview of technologies, processes, issues, and options. *Mar. Pollut. Bull.* **2012**, *65*, 23–27. [[CrossRef](#)]
13. Moreno-Madriñán, M.J.; Rickman, D.L.; Ogashawara, I.; Irwin, D.E.; Ye, J.; Al-Hamdan, M.Z. Using remote sensing to monitor the influence of river discharge on watershed outlets and adjacent coral Reefs: Magdalena River and Rosario Is-lands, Colombia. *Int. J. Appl. Earth Obs. Geoinf.* **2015**, *38*, 204–215.
14. Nellemann, C.; Hain, S.; Alde, R.J. *Dead Water: Merging of Climate Change with Pollution, Over-Harvest, and Infestations in the World's Fishing Grounds*; United Nations Environment Programme: Arendal, Norway, 2008.
15. Caballero, I.; Fernández, R.; Escalante, O.M.; Mamán, L.; Navarro, G. New capabilities of Sentinel-2A/B satellites combined with in situ data for monitoring small harmful algal blooms in complex coastal waters. *Sci. Rep.* **2020**, *10*, 8743.
16. Shamsudeen, T.Y. Advances in remote sensing technology, machine learning and deep learning for marine oil spill detection, prediction and vulnerability assessment. *Remote Sens.* **2020**, *12*, 3416.
17. Katlane, R.; Dupouy, C.; El Kilani, B.; Berges, J.C. Estimation of Chlorophyll and Turbidity Using Sentinel 2A and EO1 Data in Kneiss Archipelago Gulf of Gabes, Tunisia. *Int. J. Geosci.* **2020**, *11*, 708–728. [[CrossRef](#)]
18. Themistocleous, K.; Papoutsas, C.; Michaelides, S.; Hadjimitsis, D. Investigating Detection of Floating Plastic Litter from Space Using Sentinel-2 Imagery. *Remote Sens.* **2020**, *12*, 2648. [[CrossRef](#)]
19. Ambade, B.; Sethi, S.S.; Chintalacheruvu, M.R. Distribution, risk assessment, and source apportionment of polycyclic aromatic hydrocarbons (PAHs) using positive matrix factorization (PMF) in urban soils of East India. *Environ. Geochem. Health* **2022**, *45*, 491–505. [[CrossRef](#)]
20. Liu, H.L.; Nie, H.T.; Wang, Y.L.; Sun, X.; Wei, H. Estimation method of pollutant load into sea using statistical data—Tianjin city. *Mar. Environ. Sci.* **2019**, *38*, 968–976.
21. Kurwadkar, S.; Sankar, T.K.; Kumar, A.; Ambade, B.; Gautam, S.; Gautam, A.S.; Biswas, J.K.; Salam, M.A. Emissions of black carbon and polycyclic aromatic hydrocarbons: Potential implications of cultural practices during the Covid-19 pandemic. *Gondwana Res.* **2023**, *114*, 4–14. [[CrossRef](#)]
22. Ge, H.Q.; Lan, N. Causes and Prevention Mode on Marine Pollution from the Land-based Activities or Sources (MPLBA) in China. *China Soft Sci.* **2014**, *2*, 22–31.
23. Ma, X.D.; Mu, J.L.; Lin, Z.S.; Wang, L.J.; Yu, L.M.; Wang, Y.; Zhang, Z.; Zhang, Z.F. The Impact of Sewage from Typical Land-based Sources on the Adjacent Marine Eutrophication and Biological Toxicity. *Environ. Monitor. China* **2014**, *30*, 25–30.
24. Xu, L.H.; Li, J.L.; Li, W.F.; Zhao, S.; Yuan, Q.X.; Wang, M.Y.; Yang, L.; Lu, X.S. Progress in Impact of Human Activities on Coastal Resource and Environment. *J. Nanjing Univ. Nat. Sci. Ed.* **2014**, *37*, 124–131.

25. Davenport, J.; Davenport, J.L. The impact of tourism and personal leisure transport on coastal environments: A review. *Estuar. Coast. Shelf Sci.* **2006**, *67*, 280–292.
26. GB 3097-1997; Marine Water Quality Standard. State Environmental Protection Administration: Beijing, China, 1997.
27. GB 3838-2002; Environmental Quality Standards for Surface Water. State Environmental Protection Administration (SEPA): Beijing, China; General Administration of Quality Supervision, Inspection and Quarantine (AQSIQ) of the People's Republic of China: Beijing, China, 2002.
28. Chen, Y.B.; Song, G.B.; Zhao, W.X.; Chen, J.W. Estimating pollutant loadings from mariculture in China. *Mar. Environ. Sci.* **2016**, *35*, 1–6.
29. Liu, J.L.; Chen, X.J. Research Progress and Hotspots of Marine Biodiversity: Based on Bibliometrics and Knowledge Mapping Analysis. *Prog. Fish. Sci.* **2021**, *42*, 201–213.
30. Wang, C.Y.; He, S.J.; Li, Y.T.; Hou, X.Y.; Yang, C.Y. Study on the state and ecological effect of spilled oil pollution in Chinese Coastal Waters. *Mar. Sci.* **2009**, *33*, 57–60.
31. GB 11607-1989; Water Quality Standard for Fisheries. State Environmental Protection Administration: Beijing, China, 1989.
32. GB/T 17108-2006; Technical Directives for the Division of Marine Functional Zonation. General Administration of Quality Supervision, Inspection and Quarantine (AQSIQ): Beijing, China; Standardization Administration of the People's Republic of China (SAC): Beijing, China, 2006.
33. Kumar, A.; Ambade, B.; Sankar, T.K.; Sethi, S.S.; Kurwadkar, S. Source identification and health risk assessment of atmospheric PM_{2.5}-bound polycyclic aromatic hydrocarbons in Jamshedpur, India. *Sustain. Cities Soc.* **2019**, *52*, 101801.
34. Ambade, B.; Kumar, A.; Latif, M. Emission sources, Characteristics and risk assessment of particulate bound Polycyclic Aromatic Hydrocarbons (PAHs) from traffic sites. 2021, *preprint*.
35. Lin, M.S.; He, X.Q.; Jia, Y.J.; Bai, Y.; Ye, X.M.; Gong, F. Advances in marine satellite remote sensing technology in China. *Acta Oceanol. Sin.* **2019**, *41*, 99–112.
36. Wang, W.J.; Jia, D.N.; Xu, J.L.; Chu, H.K.; Dong, X.R. Review of the development of global marine remote sensing satellite. *Bull. Surv. Mapp.* **2020**, *5*, 1–6.
37. Baig, M.H.A.; Zhang, L.; Shuai, T.; Tong, Q. Derivation of a tasselled cap transformation based on Landsat 8 at-satellite reflectance. *Remote Sens. Lett.* **2014**, *5*, 423–431. [[CrossRef](#)]
38. Blix, K.; Pálffy, K.; Tóth, V.R.; Eltoft, T. Remote sensing of water quality parameters over Lake Balaton by using sentinel-3 OLCI. *Water* **2018**, *10*, 1428.
39. Atlas, R.; Hoffman, R.N.; Ardizzone, J.; Leidner, S.M.; Jusem, J.C.; Smith, D.K.; Gombos, D. A cross-calibrated multi-platform ocean surface wind velocity product for meteorological oceanographic applications. *Bull. Am. Meteorol. Soc.* **2011**, *92*, 157–174. [[CrossRef](#)]
40. Su, H.; Li, W.; Yan, X. Retrieving temperature anomaly in the global subsurface deeper ocean from satellite observations. *J. Geophys. Res. Ocean.* **2018**, *123*, 399–410.
41. Sun, W.W.; Yang, G.; Chen, C.; Chang, M.H.; Huang, K.; Meng, X.Z.; Liu, L.Y. Development status literature analysis of China's earth observation remote sensing satellites. *J. Remote Sens.* **2020**, *24*, 479–510. [[CrossRef](#)]
42. Jiang, X.W.; Lin, M.S.; Liu, J.Q.; Zhang, Y.Q.; Xie, X.T.; Peng, H.L.; Zhou, W. The HY-2 satellite its preliminary assessment. *Int. J. Digit. Earth* **2012**, *5*, 266–281. [[CrossRef](#)]
43. Zhao, C.; Jia, M.; Wang, Z.; Mao, D.; Wang, Y. Toward a better understanding of coastal salt marsh mapping: A case from China using dual-temporal images. *Remote Sens. Environ.* **2023**, *295*, 113664. [[CrossRef](#)]
44. Dmytro, K.; Susanne, K. Evaluation of sentinel-3A OLCI products derived using the case-2 regional coast colour processor over the Baltic Sea. *Sensors* **2019**, *19*, 3609.
45. Wang, J.T.; Xu, X.G.; Meng, X.H. The modified ensemble empirical mode decomposition method and extraction of oceanic internal wave from synthetic aperture radar image. *J. Shanghai Jiaotong Univ. Sci.* **2015**, *20*, 243–250. [[CrossRef](#)]
46. Chen, C.; Yuxi, S.; Jun, T. Research on Marine Disaster Prevention and Mitigation Information Platform System Based on Big Data. *IOP Conf. Ser. Earth Environ. Sci.* **2021**, *632*, 022082. [[CrossRef](#)]
47. Yu, G.; Yang, W.; Matsushita, B.; Li, R.; Oyama, Y.; Fukushima, T. Remote Estimation of Chlorophyll-a in Inland Waters by a NIR-Red-Based Algorithm: Validation in Asian Lakes. *Remote Sens.* **2014**, *6*, 3492–3510. [[CrossRef](#)]
48. Masoud, A.A. On the Retrieval of the Water Quality Parameters from Sentinel-3/2 and Landsat-8 OLI in the Nile Delta's Coastal and Inland Waters. *Water* **2022**, *14*, 593.
49. Giorgio, D.; Anatoly, A.G. Effect of bio-optical parameter variability and uncertainties in reflectance measurements on the remote estimation of chlorophyll-a concentration in turbid productive waters: Modeling results. *Appl. Opt.* **2005**, *45*, 3577–3592.
50. Mao, Z.; Chen, J.; Pan, D.; Tao, B.; Zhu, Q. A regional remote sensing algorithm for total suspended matter in the East China Sea. *Remote Sens. Environ.* **2012**, *124*, 819–831. [[CrossRef](#)]
51. Yin, X.Q.; Yang, D.T.; Zhou, L.Z. Estimation of suspended particulate matter transport via the boundary waters of the Yellow Sea the East Sea based on satellite remote sensing. *J. Trop. Oceanogr.* **2018**, *37*, 10–16.
52. Ahn, Y.H.; Shanmugam, P. Detecting the red tide algal blooms from satellite ocean color observations in optically complex Northeast-Asia Coastal waters. *Remote Sens. Environ.* **2006**, *103*, 419–437. [[CrossRef](#)]
53. Hu, C.; Barnes, B.B.; Qi, L.; Corcoran, A.A. A Harmful Algal Bloom of *Karenia brevis* in the Northeastern Gulf of Mexico as Revealed by MODIS and VIIRS: A Comparison. *Sensors* **2015**, *15*, 2873–2887. [[CrossRef](#)] [[PubMed](#)]

54. Zhang, H.; Zheng, X.S. Study on red tide remote sensing monitoring in the Bohai Sea in 2014. *Mar. Sci. Bull.* **2017**, *19*, 37–51.
55. Jiang, X.W.; He, X.Q.; Lin, M.S.; Gong, F.; Ye, X.M.; Pan, D.L. Progresses on ocean satellite remote sensing application in China. *Acta Oceanol. Sin.* **2019**, *41*, 113–124.
56. Pan, D.; He, X.; Mao, T. Preliminary study on the orbit cross-calibration of CMODIS by SeaWiFS. *Prog. Nat. Sci.* **2003**, *13*, 745–749. [[CrossRef](#)]
57. Pan, Y.Y.; Guo, Q.X.; Sun, Y.H. Advances in remote sensing inversion method of chlorophyll a concentration. *Sci. Surv. Mapp.* **2017**, *42*, 43–48.
58. Zhao, J.; Ghedira, H. Monitoring red tide with satellite imagery and numerical models: A case study in the Arabian Gulf. *Mar. Pollut. Bull.* **2014**, *79*, 305–313. [[CrossRef](#)]
59. Harvey, B.P.; Gwynn-Jones, D.; Moore, P.J. Meta-analysis reveals complex marine biological responses to the interactive effects of ocean acidification and warming. *Ecol. Evol.* **2013**, *3*, 1016–1030. [[CrossRef](#)] [[PubMed](#)]
60. Caballero, I.; Stumpf, P.R.; Meredith, A. Preliminary assessment of turbidity and chlorophyll impact on bathymetry de-rived from sentinel-2A and sentinel-3A satellites in South Florida. *Remote Sens.* **2019**, *11*, 645.
61. Girolametti, F.; Fanelli, M.; Ajdini, B.; Truzzi, C.; Illuminati, S.; Susmel, S.; Celussi, M.; Šangulin, J.; Annibaldi, A. Dissolved Potentially Toxic Elements (PTEs) in Relation to Depuration Plant Outflows in Adriatic Coastal Waters: A Two Year Monitoring Survey. *Water* **2022**, *14*, 569. [[CrossRef](#)]
62. Yang, Y.P.; Wang, Q.; Wang, W.J.; Gao, S.P. Application and Advances of Remote Sensing Techniques in Determining Water Quality. *Geogr. Geo-Inf. Sci.* **2004**, *6*, 6–12.
63. Shang, S.; Lee, Z.; Wei, G. Characterization of MODIS-derived euphotic zone depth: Results for the China Sea. *Remote Sens. Environ.* **2011**, *115*, 180–186. [[CrossRef](#)]
64. Farré, M. Remote and in situ devices for the assessment of marine contaminants of emerging concern and plastic debris detection. *Curr. Opin. Environ. Sci. Health* **2020**, *18*, 79–94. [[CrossRef](#)]
65. Lu, X.M.; Su, H. Retrieving total suspended matter concentration in Fujian coastal waters using OLCI data. *Acta Sci. Circumstantiae* **2020**, *40*, 2819–2827.
66. Hou, L.L.; Ma, A.Q.; Hu, J.; Shan, G.Y.; Deng, J.M.; Han, J.Y.; Ding, Z.Y. Study on Remote Sensing Retrieval Model Optimization of Suspended Sediment Concentration in Jiaozhou Bay. *Period. Ocean Univ. China* **2018**, *48*, 98–108.
67. Ahn, J.-H.; Park, Y.-J.; Ryu, J.-H.; Lee, B.; Oh, I.S. Development of atmospheric correction algorithm for Geostationary Ocean Color Imager (GOCI). *Ocean Sci. J.* **2012**, *47*, 247–259. [[CrossRef](#)]
68. Ryu, J.-H.; Han, H.-J.; Cho, S.; Park, Y.-J.; Ahn, Y.-H. Overview of geostationary ocean color imager (GOCI) and GOCI data processing system (GDPS). *Ocean Sci. J.* **2012**, *47*, 223–233. [[CrossRef](#)]
69. Zheng, X.S.; Zhang, Y.N.; Liu, X.H. Research on inversion method of aerosol optical depth over the Yellow Sea based on GOCI data. *Mar. Sci. Bull.* **2020**, *39*, 94–100.
70. Chen, J.; Quan, W.; Cui, T.; Song, Q. Estimation of total suspended matter concentration from MODIS data using a neural network model in the China eastern coastal zone. *Estuar. Coast. Shelf Sci.* **2015**, *155*, 104–113. [[CrossRef](#)]
71. Tian, H.Z.; Liu, Q.P.; Goes, J.I.; Gomes, H.D.R.; Yang, M.M. Temporal and spatial changes in chlorophyll-a concentrations in the Yellow Sea from 2002 to 2018 based on MODIS data. *Mar. Sci. Bull.* **2020**, *39*, 101–110.
72. Yu, G.; Fu, D.Y.; Zhong, Y.F.; Liu, D.Z.; Qi, Y.L.; Lou, Y.F. Remote Sensing Retrieval of Colored Dissolved Organic Matter in Zhanjiang Coastal Area. *J. Guangdong Ocean Univ.* **2021**, *41*, 55–62.
73. Wang, L.; Zhao, D.Z.; Yang, J.H.; Chen, Y.L. The optical properties and remote sensing retrieval model of chromophoric dissolved organic matter in the Dayang Estuary. *Acta Oceanol. Sin.* **2011**, *33*, 45–51.
74. David, O.; Anjan, D. Institutional and Policy Cocktails for Protecting Coastal and Marine Environments from Land-based Sources of Pollution. *Ocean Coast. Manag.* **2006**, *49*, 576–596.
75. Huisman, J.; Codd, G.A.; Paerl, H.W.; Paerl, H.W.; Ibelings, B.W.; Verspagen, J.M.H.; Visser, P.M. Cyanobacterial blooms. *Nature reviews. Microbiology* **2018**, *6*, 471–483.
76. Inia, M.S.; Jennifer, C.; Frank, E.M.K.; Hu, C.M.; Jennifer, W.; Dmitry, G. Evaluation and optimization of remote sensing techniques for detection of *Karenia brevis* blooms on the West Florida Shelf. *Remote Sens. Environ.* **2015**, *170*, 239–254.
77. Kutser, T.; Metsamaa, L.; Dekker, A.G. Influence of the vertical distribution of cyanobacteria in the water column on the remote sensing signal. *Estuar. Coast. Shelf Sci.* **2008**, *78*, 649–654. [[CrossRef](#)]
78. Hu, C. A novel ocean color index to detect floating algae in the global oceans. *Remote Sens. Environ.* **2009**, *113*, 2118–2129. [[CrossRef](#)]
79. Tao, B.; Pan, D.; Mao, Z.; Shen, Y.; Zhu, Q.; Chen, J. Optical detection of *Prorocentrum donghaiense* blooms based on multispectral reflectance. *Acta Oceanol. Sin.* **2013**, *32*, 48–56. [[CrossRef](#)]
80. Gower, J.; King, S.; Wei, Y.; Borstad, G.; Brown, L. Use of the 709 nm band of MERIS to detect intense plankton blooms and other conditions in coastal waters. In Proceedings of the MERIS User Workshop, Frascati, Italy, 10–13 November 2003; pp. 10–13.
81. Lee, Z.; Carder, K.L.; Arnone, R. Deriving inherent optical properties from water color: A multiband quasi-analytical algorithm for optically deep waters. *Appl. Opt.* **2002**, *41*, 5755–5772.
82. Li, X.; Liu, B.; Zheng, G.; Ren, Y.; Zhang, S.; Liu, Y.; Gao, L.; Liu, Y.; Zhang, B.; Wang, F. Deep-learning-based information mining from ocean remote-sensing imagery. *Natl. Sci. Rev.* **2020**, *7*, 1584–1605. [[CrossRef](#)] [[PubMed](#)]

83. Hu, C.; Li, X.; William, G.P.; Frank, E.M.K. Detection of natural oil slicks in the NW Gulf of Mexico using MODIS imagery. *Geophys. Res. Lett.* **2009**, *36*, L01604.
84. Hu, C.; Muller-Karger, F.E.; Taylor, C.; Carder, K.L.; Kelble, C.; Johns, E.; Heil, C.A. Red tide detection and tracing using MODIS fluorescence data: A regional example in SW Florida coastal waters. *Remote Sens. Environ.* **2005**, *97*, 311–321. [[CrossRef](#)]
85. Shi, W.; Wang, M. Green macroalgae blooms in the Yellow Sea during the spring and summer of 2008. *J. Geophys. Res. Atmos.* **2009**, *114*. [[CrossRef](#)]
86. Xing, Q.; Hu, C. Mapping macroalgal blooms in the Yellow Sea and East China Sea using HJ-1 and Landsat data: Application of a virtual baseline reflectance height technique. *Remote Sens. Environ.* **2016**, *178*, 113–126.
87. Shuo, H.E.; Lou, X.L.; Shi, A.Q.; Li, D.L.; Wang, J.; Zhang, H.G. Simulation and Study of Remote Sensing Reflectance Spectra of Typical Algal Blooms in the East China Sea. *Oceanol. Limnol. Sin.* **2019**, *50*, 525–531.
88. Zhang, H.L.; Sun, D.Y.; Li, J.S.; Qiu, Z.F.; Wang, S.Q.; He, Y.J. Remote Sensing Algorithm for Detecting Green Tide in China Coastal Waters Based on GF1-WFV and H-CCD Data. *Acta Opt. Sin.* **2016**, *36*, 36–44.
89. Chen, Y.; Sun, D.Y.; Zhang, H.L.; Wang, S.Q. Remote-Sensing Monitoring of Green Tide and Its Drifting Trajectories in Yellow Sea Based on Observation Data of Geostationary Ocean Color Imager. *Acta Opt. Sin.* **2020**, *40*, 0301001. [[CrossRef](#)]
90. Son, Y.B.; Min, J.-E.; Ryu, J.-H. Detecting massive green algae (*Ulva prolifera*) blooms in the Yellow Sea and East China Sea using Geostationary Ocean Color Imager (GOCI) data. *Ocean Sci. J.* **2012**, *47*, 359–375. [[CrossRef](#)]
91. Zhang, H.; Qiu, Z.; Devred, E.; Sun, D.; Wang, S.; He, Y.; Yu, Y. A simple and effective method for monitoring floating green macroalgae blooms: A case study in the Yellow Sea. *Opt. Express* **2019**, *27*, 4528–4548. [[CrossRef](#)]
92. Jiang, D.J.; Wang, K.; Xia, Y. Comparative studies on remote sensing techniques for red tide monitoring in Bohai Sea. *Mar. Environ. Sci.* **2020**, *39*, 460–467.
93. Tao, B.Y.; Mao, Z.H.; Lei, H.; Pan, D.L.; Shen, Y.Z.; Bai, Y.; Zhu, Q.K.; Li, Z.E. A novel method for discriminating *Prorocentrum donghaiense* from diatom blooms in the East China Sea using MODIS measurements. *Remote Sens. Environ.* **2015**, *158*, 267–280.
94. Kim, Y.; Byun, Y.; Kim, Y.; Eo, Y. Detection of *Cochlodinium polykrikoides* red tide based on two-stage filtering using MODIS data. *Desalination* **2009**, *249*, 1171–1179. [[CrossRef](#)]
95. Liu, F.; Chen, C.; Tang, S.; Liu, D. Retrieval of chlorophyll concentration from the enveloped areas of fluorescence spectra in Pearl River estuary, China. *Proc. SPIE-Int. Soc. Opt. Eng.* **2010**, *64*, 1912–1916.
96. Commendatore, M.G.; Esteves, J.L. An Assessment of Oil Pollution in the Coastal Zone of Patagonia, Argentina. *Environ. Manag.* **2007**, *40*, 814–821. [[CrossRef](#)]
97. Zou, Y.; Zou, B.; Liang, C.; Cui, S.; Zeng, T. Multiple Index Information Extraction of Marine Oil Spills. *Geo-Inf. Sci.* **2012**, *14*, 265–269. [[CrossRef](#)]
98. Nirchio, F.; Sorgente, M.; Giancaspro, A.; Biamino, W.; Parisato, E.; Ravera, R.; Trivero, P. Automatic detection of oil spills from SAR images. *Int. J. Remote Sens.* **2005**, *26*, 1157–1174. [[CrossRef](#)]
99. Lu, Y.; Li, X.; Tian, Q.J.; Zheng, G.; Sun, S.J.; Liu, Y.X.; Yang, Q. Progress in marine oil spill optical remote sensing: Detected targets, spectral response characteristics, and theories. *Mar. Geod.* **2013**, *36*, 334–346.
100. Yu, L.; Jonathan, L. Oil spill detection from SAR intensity imagery using a marked point process. *Remote Sens. Environ.* **2010**, *114*, 1590–1601.
101. Zhang, B.; Perrie, W.; Li, X.; Pichel, W.G. Mapping sea surface oil slicks using RADARSAT-2 quad-polarization SAR image. *Geophys. Res. Lett.* **2011**, *38*, 415–421. [[CrossRef](#)]
102. Lu, Y.; Zhan, W.; Hu, C. Detecting and quantifying oil slick thickness by thermal remote sensing: A ground-based experiment. *Remote Sens. Environ.* **2016**, *181*, 207–217.
103. Wettle, M.; Daniel, P.J.; Logan, G.A.; Thankappan, M. Assessing the effect of hydrocarbon oil type and thickness on a remote sensing signal: A sensitivity study based on the optical properties of two different oil types and the HYMAP and Quickbird sensors. *Remote Sens. Environ.* **2009**, *113*, 2000–2010. [[CrossRef](#)]
104. Huang, K.; Pan, Q.; Zhang, J.Y.; Wang, Y.L.; Yang, G.; Sun, W.W. Quantitative monitoring in oil spill incidents based on GF-1 satellite: Qingdao oil spill accident case. *Mar. Sci. Bull.* **2020**, *39*, 266–271.
105. Lu, Y.C.; Liu, J.Q.; Ding, J.; Shi, J.; Chen, J.Y.; Ye, X.M. Optical remote identification of spilled oils from the SANCHI oil tanker collision in the East China Sea. *Chin. Sci. Bull.* **2019**, *64*, 3213–3222.
106. Solberg, A.H.S.; Brekke, C.; Husoy, P.O. Oil Spill Detection in Radarsat and Envisat SAR Images. *IEEE Trans. Geosci. Remote Sens.* **2007**, *45*, 746–755. [[CrossRef](#)]
107. Jiao, J.; Lu, Y.; Hu, C.; Shi, J.; Sun, S.; Liu, Y. Quantifying ocean surface oil thickness using thermal remote sensing. *Remote Sens. Environ.* **2021**, *261*, 112513. [[CrossRef](#)]
108. Shen, Y.F.; Liu, J.Q.; Ding, J.; Jiao, J.N.; Sun, S.J.; Lu, Y.C. HY-1C COCTS and CZI observation of marine oil spills in the South China Sea. *J. Remote Sens.* **2020**, *24*, 933–944. [[CrossRef](#)]
109. Zou, Y.R.; Liang, C.; Chen, J.L.; Cui, S.X.; Lang, S.Y. An optimal parametric analysis of monitoring oil spill based on SAR. *Acta Ocean. Sin.* **2011**, *33*, 36–44.
110. Hu, C. Remote detection of marine debris using satellite observations in the visible and near infrared spectral range: Challenges and potentials. *Remote Sens. Environ.* **2021**, *259*, 112414. [[CrossRef](#)]
111. Kikaki, A.; Karantzalos, K.; Power, C.A.; Raitos, D.E. Remotely Sensing the Source and Transport of Marine Plastic Debris in Bay Islands of Honduras (Caribbean Sea). *Remote Sens.* **2016**, *12*, 1727.

112. Lauren, B.; Daniel, C.; Victor, M.V.; Konstantinos, T. Finding Plastic Patches in Coastal Waters using Optical Satellite Data. *Sci. Rep.* **2020**, *10*, 5364.
113. Paul, M.S.H.; John, B.; Carme, A.; Montserrat, C.; Laia, R.; Salud, D. Assessment of marine litter through remote sensing: Recent approaches and future goals. *Mar. Pollut. Bull.* **2021**, *168*, 112347.
114. Lonneke, G.M.; Steef, P.; Erik, V.S.; James, N.A.; Stuart, G. Concept for a hyperspectral remote sensing algorithm for floating marine macro plastics. *Mar. Pollut. Bull.* **2018**, *126*, 255–262.
115. Topouzelis, K.; Papageorgiou, D.; Suaria, G.; Aliani, S. Floating marine litter detection algorithms and techniques using optical remote sensing data: A review. *Mar. Pollut. Bull.* **2021**, *170*, 112675. [[CrossRef](#)]
116. Martin, C.; Parkes, S.; Zhang, Q.; Zhang, X.; McCabe, M.F.; Duarte, C.M. Use of unmanned aerial vehicles for efficient beach litter monitoring. *Mar. Pollut. Bull.* **2018**, *131*, 662–673. [[CrossRef](#)]
117. Hamilton, B.; Dean, C.; Kurata, N.; Vella, K.; Soloviev, A.; Tartar, A.; Shivji, M.; Matt, S.; Perrie, W.; Lehner, S.; et al. Surfactant Associated Bacteria in the Sea Surface Microlayer: Case Studies in the Straits of Florida and the Gulf of Mexico. *Can. J. Remote Sens.* **2015**, *41*, 135–143. [[CrossRef](#)]
118. Aoyama, T. Extraction of marine debris in the Sea of Japan using high-spatial-resolution satellite images. In *Remote Sensing of the Oceans and Inland Waters: Techniques, Applications, and Challenges*; SPIE: New Delhi, India, 2016.
119. Kurata, N.; Vella, K.; Hamilton, B.; Shivji, M.; Soloviev, A.; Matt, S.; Tartar, A.; Perrie, W. Surfactant-associated bacteria in the near-surface layer of the ocean. *Sci. Rep.* **2016**, *6*, srep19123. [[CrossRef](#)]
120. Davaasuren, N.; Marino, A.; Boardman, C.P.; Alparone, M.; Nunziat, F.; Ackermann, N.; Hajnsek, I. Detecting Micro-plastics Pollution in World Oceans Using Sar Remote Sensing. In Proceedings of the IGARSS 2018-2018 IEEE International Geoscience and Remote Sensing Symposium, Valencia, Spain, 22–27 July 2018; pp. 938–941.
121. Howe, K.L.; Dean, C.W.; Kluge, J.; Soloviev, A.V.; Tartar, A.; Shivji, M.; Lehner, S.; Perrie, W. Relative abundance of *Bacillus* spp., surfactant-associated bacterium present in a natural sea slick observed by satellite SAR imagery over the Gulf of Mexico. *Elem. Sci. Anthr.* **2018**, *6*, 8. [[CrossRef](#)]
122. Mao, Y.; Zheng, J.L.; Qiu, Z.F.; Muhammad, B. Precision analysis and spatiotemporal distribution characteristics from multi source satellite aerosol optical depth data in the Yellow Sea and Bohai Sea. *Acta Sci. Circumstantiae* **2021**, *41*, 2550–2559.
123. Veefkind, J.; de Leeuw, G.; Stammes, P.; Koelemeijer, R.B. Regional Distribution of Aerosol over Land, Derived from ATSR-2 and GOME. *Remote Sens. Environ.* **2000**, *74*, 377–386. [[CrossRef](#)]
124. Dong, H.Y.; Liu, Y.; Guan, Z.Y. Validation of MODIS Aerosol Optical Depth Retrievals over East China Sea. *J. Nanjing Inst. Meteorol.* **2007**, *3*, 328–337.
125. Lee, J.; Kim, J.; Song, C.H.; Ryu, J.-H.; Ahn, Y.-H. Algorithm for retrieval of aerosol optical properties over the ocean from the Geostationary Ocean Color Imager. *Remote Sens. Environ.* **2010**, *114*, 1077–1088. [[CrossRef](#)]
126. Lin, M.S.; Ye, X.M.; Yuan, X.Z. The first quantitative joint observation of typhoon by Chinese GF-3 SAR and HY-2A microwave scatterometer. *Acta Oceanol. Sin.* **2017**, *36*, 1–3. [[CrossRef](#)]
127. Wang, S.; Feng, H.H.; Zou, B.; Yang, Z.L.; Ding, Y.; Ye, S.C.; Zhu, S.J. Research progresses on deposition monitoring of air pollution. *China Environ. Sci.* **2021**, *41*, 4961–4972.
128. Hao, Z.Z.; Pan, D.L.; Bai, Y. Characteristics of the spatial distribution monthly variation of aerosol optical thickness derived from SeaWiFS over the China Seas. *J. Mar. Sci.* **2007**, *s98*, 80–87.
129. Kachelriess, D.; Wegmann, M.; Gollock, M.; Pettorelli, N. The application of remote sensing for marine protected area management. *Ecol. Indic.* **2014**, *36*, 169–177. [[CrossRef](#)]
130. Su, H.; Liu, H.; Heyman, W.D. Automated Derivation of Bathymetric Information from Multi-Spectral Satellite Imagery Using a Non-Linear Inversion Model. *Mar. Geod.* **2008**, *31*, 281–298. [[CrossRef](#)]
131. Wu, Z.Q.; Mao, Z.H.; Wang, Z.; Qiu, Y.W.; Shen, W. Research on Remote Sensing Inversion of Shallow Water Depth Based on Extreme Learning Machine. *Hydrogr. Surv. Charting* **2019**, *39*, 11–15.
132. Franz, B.A.; Bailey, S.W.; Werdell, P.J.; McClain, C.R. Sensor-independent approach to the vicarious calibration of satellite ocean color radiometry. *Appl. Opt.* **2007**, *46*, 5068–5082. [[CrossRef](#)] [[PubMed](#)]

Disclaimer/Publisher’s Note: The statements, opinions and data contained in all publications are solely those of the individual author(s) and contributor(s) and not of MDPI and/or the editor(s). MDPI and/or the editor(s) disclaim responsibility for any injury to people or property resulting from any ideas, methods, instructions or products referred to in the content.